Wind-Induced Baroclinic Motions at the Edge of the Continental Shelf[1]

G. T. CSANADY[2]

Woods Hole Oceanographic Institution, Woods Hole, Mass. 02543

(Manuscript received 19 February 1973, in revised form 9 April 1973)

ABSTRACT

In a two-layer model of stratified fluid flow, motions in the internal mode are governed by the distribution of an *equivalent* depth h_e. For a typical continental shelf, the distribution of h_e with distance from shore may be closely approximated by two straight-line distributions patched at the shelf break, one of constant slope and one of constant (equivalent) depth. For such a simple model the *forced* response to a suddenly imposed wind stress (in the internal mode) is easily calculated. The component of the wind stress perpendicular to shore produces a step-like feature of the thermocline at the shelf, and a longshore Ekman drift gradually reducing to zero at the coast from the infinite ocean value far offshore. Wind stress parallel to the shore produces a thermocline step and a longshore jet at the shelf break, both of linearly increasing amplitude (in time), and an onshore or offshore Ekman drift, again reducing to zero at the coast but having the infinite-ocean magnitude far offshore.

1. Introduction

One would expect water movements over continental shelves to exhibit at least some similarities with those in large, oblong lakes, such as, for example, Lake Michigan. The width and depth scales are quite similar, and the seasonal thermocline (or rather pycnocline) occurs at comparable depths, with a very similar density jump across it. The main difference is that one edge of the shelf is open to the deep sea: at this open edge a rather extreme and abrupt depth increase terminates the shelf, providing a boundary condition quite different from an opposing shore.

It has by now been well documented that the seasonal thermocline is subject to relatively very large wind-induced displacements within the coastal boundary layer of large lakes. The resulting coastal upwelling or downwelling of the thermocline is often (although not always) accompanied by a baroclinic coastal jet. The simplest dynamical theory which reproduces these phenomena relies on the linearized equations of motion, takes into account stratification by a two-layer model, and contains a constant Coriolis parameter. The wind stress may be highly idealized, e.g., assumed constant in space, if it is allowed to vary in time at least to the extent that it is suddenly imposed. Basin topography may also be highly idealized: a circular basin or a long and narrow lake model lead to very similar coastal responses (Csanady, 1973). Frictional forces appear to cause only relatively straightforward damping effects near solid boundaries and may be neglected in a first approximation. However, in a frictionless model it is necessary to consider *time-dependent* motions, both free oscillations and an accelerating forced flow pattern. Analytical models of a long and narrow lake, based on the above simplifications, are particularly simple and illuminating. The key point is perhaps that the shores prevent perpendicular water movements and thereby suppress the development of Ekman drift. Thus, when a wind stress is exerted at the lake surface, the stress component perpendicular to the shore causes a thermocline upwelling or downwelling, while the parallel component sets up both upwelling (or downwelling) *and* a baroclinic coastal jet.

The question arises, as to whether similar thermocline displacements and water movements due to wind stress impulses occur at the open edge of a continental shelf, and if so, whether these will be of sufficient amplitude to constitute an important part of motions observable over the continental slope. In view of the success in long lakes of the simple analytical models, it appears to be profitable to discuss this question with their aid. The calculations below show that thermocline steps and "shelf jets" indeed occur over the shelf break, but that they are about an order of magnitude less intense than the coastal kind.

Theoretical studies of shelf dynamics, by means of numerical modeling, have recently been published by O'Brien and his collaborators, notably O'Brien and Hurlburt (1972), Hurlburt and Thompson (1973), and Thompson and O'Brien (1973). These are based on theoretical assumptions much as enumerated above, but they also take into account internal and bottom friction. Shelf topography is modeled by a step-like feature in the depth distribution. The results show thermocline features and shelf jets much as in the present

[1] Contribution No. 2644 Woods Hole Oceanographic Institution.
[2] On leave from University of Waterloo, Ontario, Canada.

calculation, in spite of rather different assumptions on the details of the depth distribution. The present study therefore helps confirm the generality of those numerical results, and, being analytical, perhaps identifies the physical factors involved somewhat more clearly. Some experimental evidence in support of the numerical results has been quoted in the above three papers of O'Brien *et al.* Further evidence is mentioned below, although it must be pointed out that the total empirical knowledge of phenomena at the shelf break is rather weak.

2. A continental shelf model

We shall be discussing *internal mode motions only* and represent the stratification of the water mass by a two-layer model. The physical situation we are considering and the coordinate system used are illustrated in Fig. 1, where the x axis coincides with the intersection of the equilibrium thermocline surface and the bottom. The proportionate density defect, $\epsilon=(\rho'-\rho)/\rho'$, has a typical value of 3×10^{-3}. For such small density contrasts, motions in the internal mode are characterized by vanishing total transport (to order ϵ):

$$\left.\begin{aligned} U+U'&=0\\ V+V'&=0\end{aligned}\right\}, \tag{1}$$

where (U,V) are depth-integrated velocities in the top layer, and (U',V') those in the bottom layer, along the x and y axes, respectively. Supposing the thermocline displacements from equilibrium, ζ', to be small compared to both h and h', and the bottom slope dh'/dy sufficiently gentle for the hydrostatic approximation to be valid, the equations of motion and continuity for the *internal* mode become (Csanady, 1971):

$$\left.\begin{aligned} \frac{\partial U}{\partial t}-fV&=g\epsilon\frac{hh'}{h+h'}\frac{\partial\zeta'}{\partial x}+\frac{h'}{h+h'}F_x\\ \frac{\partial V}{\partial t}+fU&=g\epsilon\frac{hh'}{h+h'}\frac{\partial\zeta'}{\partial y}+\frac{h'}{h+h'}F_y\\ \frac{\partial U}{\partial x}+\frac{\partial V}{\partial y}&=\frac{\partial\zeta'}{\partial t}\end{aligned}\right\}, \tag{2}$$

where F_x and F_y are wind stress components, the interface and bottom stresses having been set zero. Clearly, the linearization of the pressure gradient does not apply near $y=0$ where h' reduces to zero, and the hydrostatic approximation may also break down over a very steep continental slope. Making due allowance for these weaknesses of the simple theory, it is still likely to provide considerable physical insight into the dynamics of wind-induced motions over continental shelves, given its success in dealing with similar phenomena in long lakes.

The factor multiplying the pressure gradient terms in Eq. (2) contains the "equivalent depth" h_e, defined as

$$h_e=\frac{hh'}{h+h'}, \tag{3}$$

which is a slowly varying function of the position coordinates. To gain an idea of its typical behavior, consider, for example, the section of the sea floor just off the Virginia-Maryland border, roughly perpendicular to the coast (Fig. 2, top). The summer thermocline is typically at a depth of 20 m, so that the equivalent depth distribution is as illustrated in Fig. 2, bottom. What strikes one at once is that the extreme depth variation at the edge of the shelf hardly affects the equivalent depth distribution. Indeed, the simple idealized distribution also shown in the figure provides a close model: h_e varying linearly between $y=0$ and 80 km from $h_e=0$ to $h_e=20$ m, beyond that $h_e=$constant. This simple model is particularly realistic near the slope region, where we are most interested in the motions generated. Near the coast a rather larger slope would make the model more realistic, but we will not concern ourselves with this.

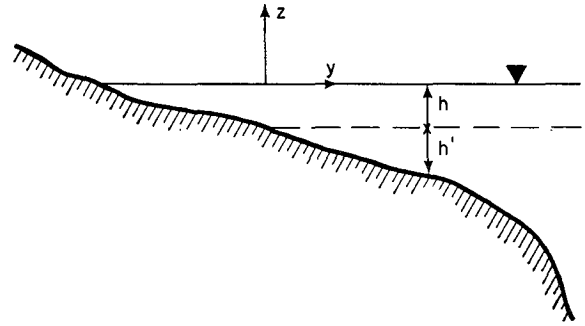

FIG. 1. Schematic illustration of continental shelf and coordinate system used.

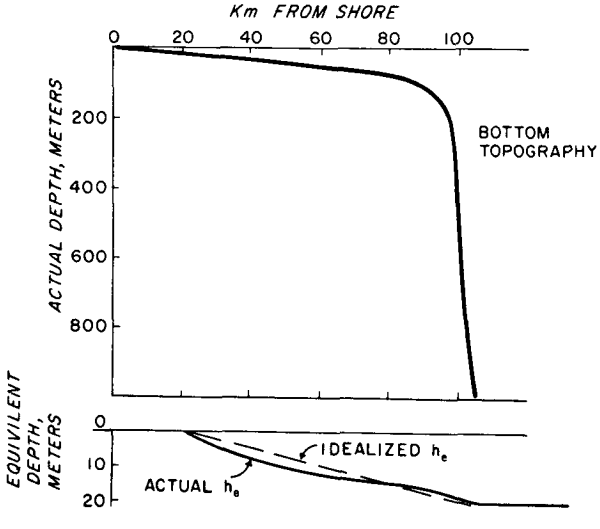

FIG. 2. Depth distribution over continental shelf off the Virginia-Maryland border (top) and the "equivalent" depth (bottom).

It is worth emphasizing here that a separate consideration of internal-mode motions on the basis of the above equations relies on the various linearizing hypotheses underlying their derivation, which are not always valid. Experimentally, it may not always be easy to abstract baroclinic components of the flow from the observed total. However, where internal-mode motions produce such large "signatures" as major thermocline displacements, theories of the kind discussed here are likely to be helpful in their understanding.

3. Response to an onshore wind

Consider now motions induced by a suddenly imposed wind on a straight, infinite shelf of the idealized equivalent depth distribution shown in Fig. 2. The response will consist of a directly forced part and of some free oscillations, much as in an infinite channel (Csanady, 1973). One may infer from the calculations of Crépon (1967) that the free oscillations will contain standing and progressive waves, all at the inertial frequency. Through the progressive waves some energy is likely to be radiated away. We shall not be concerned here with these inertial oscillations, confining our attention to the *forced* part of the response only.

Let a steady and uniform wind blow along the y axis, i.e., perpendicular to shore; $F_x=0$, $F_y=F=$constant. On an infinite shelf we may suppose x gradients to be absent, i.e.,

$$\frac{\partial \zeta'}{\partial x}=0, \quad \frac{\partial U}{\partial x}=0. \tag{4}$$

We find now from Eq. (2) after a few simple manipulations the following convenient expressions:

$$\left.\begin{aligned} \frac{\partial^2 U}{\partial t^2}-g\epsilon h_e\frac{\partial^2 U}{\partial y^2}+f^2U&=\frac{h_e}{h}fF \\ \zeta'&=\frac{1}{f}\frac{\partial U}{\partial y} \\ V&=\frac{1}{f}\frac{\partial U}{\partial t} \end{aligned}\right\}. \tag{5}$$

The second of these equations shows that potential vorticity is conserved, the reason being that the curl of $\mathbf{F}/h$ (where $\mathbf{F}$ is the wind stress vector) vanishes in this problem. The third equation demonstrates that longshore velocity is generated by the Coriolis force, in response to shoreward displacement.

In analogy with the case of an infinite channel, the forced part of the solution may be expected to be time-independent, which means $V=0$, and U satisfying

$$\frac{d^2U}{dy^2}-\frac{f^2}{g\epsilon h_e}U=-\frac{fF}{g\epsilon h}. \tag{6}$$

The idealized equivalent depth distribution is

$$\left.\begin{aligned} h_e&=sy, && y\leqslant y_0 \\ h_e&=h_{e0}=\text{constant}, && y\geqslant y_0 \end{aligned}\right\}, \tag{7}$$

where s is the slope, equal in the typical case illustrated in Fig. 2 to 2.5×10^{-4}.

The general solution of Eq. (6) over the sloping part of the shelf, $y<y_0$, is

$$U=A\lambda K_1(\lambda)+B\lambda I_1(\lambda)+\frac{sF}{fh}y, \quad y\leqslant y_0, \tag{8}$$

where A, B are constants, $K_1(\ )$ and $I_1(\ )$ are modified Bessel functions, and

$$\left.\begin{aligned} \lambda&=\left(\frac{4y}{S}\right)^{\frac{1}{2}} \\ S&=\frac{g\epsilon s}{f^2} \end{aligned}\right\}. \tag{9}$$

The quantity S is a "slope length scale." Outside the edge of the shelf the solution is

$$U=\frac{h_{e0}}{h}\frac{F}{f}+Ce^{-y/R}, \tag{10}$$

with C a constant and

$$R=\frac{(g\epsilon h_{e0})^{\frac{1}{2}}}{f}, \tag{11}$$

i.e., R is the radius of deformation in the internal mode. The solution (10) already satisfies the boundary condition at infinity:

$$\zeta'=0 \quad \text{as} \quad y\to\infty. \tag{12}$$

From the geometry of the idealized shelf we find the relationships:

$$\left.\begin{aligned} h_{e0}&=sy_0 \\ \frac{y_0}{R}&=\frac{Rf^2}{g\epsilon s}=\frac{R}{S} \\ \lambda_0&=\left(\frac{4y_0}{S}\right)^{\frac{1}{2}}=\frac{2R}{S} \end{aligned}\right\}. \tag{13}$$

For the typical case illustrated in Fig. 2, and using $\epsilon=3\times10^{-3}$ and $f=0.9\times10^{-4}$, appropriate to the latitude of the illustrated example, we find the parameters:

$$S=0.93 \text{ km}$$
$$R=8.6 \text{ km}$$
$$\lambda_0=18.5$$

In order to determine the constants A, B, C in Eqs. (8) and (10) we need three boundary conditions.

Two of these are supplied by the matching conditions at $y=y_0$, requiring continuity of ζ' and V, which by (5) also means continuity of U and dU/dy. A third boundary condition must be imposed at the shore: this relates to the normal transport V and mainly affects the value of the constant A. In the framework of the linearized theory the appropriate boundary condition is $V=0$. With the wind stress perpendicular to shore, this also means by the first of Eqs. (2) that $U=0$ at $y=0$, hence $A=0$ in Eq. (8). However, even if we set $A\neq 0$ to allow finite thermocline displacements near shore, the term $A\lambda K_1(\lambda)$ becomes very small at the shelf break where the matching conditions are applied. The reason is that $\lambda=\lambda_0=18.5$ is large compared to unity, in consequence of the particular choice of parameters in our example. It may also be seen from Eq. (13) that $\lambda_0=2y_0/R$ remains large, unless the shelf width is as narrow as one or two internal radii of deformation. Physically, the coastal upwelling/downwelling remains separate from its shelf-break analogue as long as the shelf width remains reasonably large, much as in a long lake the coastal boundary layers do not merge until the lake becomes very narrow.

Setting $A=0$, and U and dU/dy separately equal from (8) and (10), the constants B and C may be determined without difficulty and yield the following distributions of U and ζ':

$$\left.\begin{aligned}
\frac{fhU}{h_{e0}F}&=\frac{\lambda^2}{\lambda_0^2}-\frac{2\lambda}{\lambda_0^2}\frac{I_1(\lambda)}{I_0(\lambda_0)+I_1(\lambda_0)}, && y\leqslant y_0\\
\frac{fhU}{h_{e0}F}&=1-\frac{2}{\lambda_0}\frac{I_1(\lambda_0)}{I_0(\lambda_0)+I_1(\lambda_0)}\exp\left(-\frac{y-y_0}{R}\right), && y\geqslant y_0\\
\frac{f^2hR\zeta'}{h_{e0}F}&=-\frac{2}{\lambda_0}+\frac{2}{\lambda_0}\frac{I_0(\lambda)}{I_0(\lambda_0)+I_1(\lambda_0)}, && y\leqslant y_0\\
\frac{f^2hR\zeta'}{h_{e0}F}&=-\frac{2}{\lambda_0}\frac{I_1(\lambda_0)}{I_0(\lambda_0)+I_1(\lambda_0)}\exp\left(-\frac{y-y_0}{R}\right), && y\geqslant y_0
\end{aligned}\right\}. \tag{14}$$

For the rather high wind stress of 10 dyn cm^{-2} [caused by about a 40-kt (20 m sec^{-1}) wind], and using the data of the example quoted above, the response to an onshore wind is illustrated in Fig. 3, in the slope region. The top-layer longshore velocity equals the Ekman drift velocity $F/(fh)$ far offshore and reduces gradually toward the coast. The associated thermocline topography contains a step-like feature near the edge of the shelf and assumes a constant depression closer to the shore, of modest amplitude. It is of interest to note that if such a thermocline topography were observed, it would be interpreted by the dynamic height method as showing flow in the *positive x* direction, with a maximum velocity of some 3 cm sec^{-1}, as against an actual Ekman drift velocity toward *negative x* of more than 50 cm sec^{-1}.

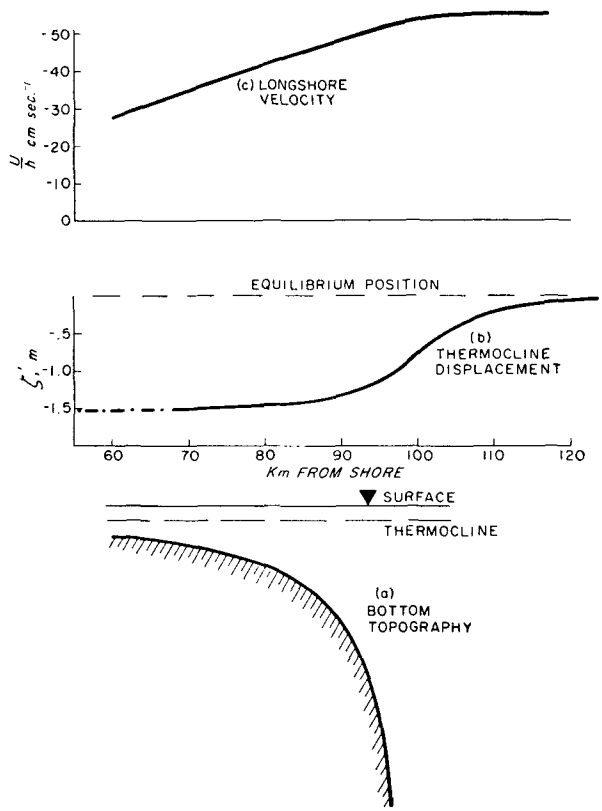

FIG. 3. Response of shelf region to onshore wind.

4. Shore-parallel wind

If the wind blows parallel to the shore ($F_x=F, F_y=0$), Eq. (2) may be reduced to the following set, again neglecting x gradients:

$$\left.\begin{aligned}
\frac{\partial^2 V}{\partial t^2}-g\epsilon h_e\frac{\partial^2 V}{\partial y^2}+f^2V&=-\frac{h_e}{h}fF\\
\frac{\partial\zeta'}{\partial t}&=\frac{\partial V}{\partial y}\\
\frac{\partial U}{\partial t}&=fV+\frac{h_e}{h}F
\end{aligned}\right\}. \tag{15}$$

In this example potential vorticity is *not* conserved, and the thermocline displacement is calculated from the divergence of the transport (which was zero in the previous example). Longshore velocity is produced by direct action of the wind stress, as well as by the Coriolis force in response to shoreward drift; the former at least must clearly yield an acceleration constant in time.

The first of Eqs. (15) is identical with the first of (5), except for the negative sign of the forcing term on the right. The matching conditions at the edge of the shelf are also the same, if expressed in terms of V, as applied to the earlier problem; namely, that V and $\partial V/\partial y$ are

continuous at $y=y_0$. Therefore, again neglecting any influence from coastal upwelling or downwelling at the edge of the shelf, the forced solution for V may be written down at once:

$$\left.\begin{aligned}\frac{fhV}{h_{e0}F} &= -\frac{\lambda^2}{\lambda_0^2}+\frac{2\lambda}{\lambda_0^2}\frac{I_1(\lambda)}{I_0(\lambda_0)+I_1(\lambda_0)}, && y\leqslant y_0\\ \frac{fhV}{h_{e0}F} &= -1+\frac{2}{\lambda_0}\frac{I_1(\lambda_0)}{I_0(\lambda_0)+I_1(\lambda_0)}\exp\left(-\frac{y-y_0}{R}\right), && y\geqslant y_0\end{aligned}\right\}. \tag{16}$$

The second and third of Eqs. (15) then immediately yield corresponding expressions for thermocline displacement and longshore transport:

$$\left.\begin{aligned}\frac{fhR\zeta'}{h_{e0}Ft} &= \frac{2}{\lambda_0}-\frac{2}{\lambda_0}\frac{I_0(\lambda)}{I_0(\lambda_0)+I_1(\lambda_0)}, && y\leqslant y_0\\ \frac{fhR\zeta'}{h_{e0}Ft} &= \frac{2}{\lambda_0}\frac{I_1(\lambda_0)}{I_0(\lambda_0)+I_1(\lambda_0)}\exp\left(-\frac{y-y_0}{R}\right), && y\geqslant y_0\\ \frac{hU}{h_{e0}Ft} &= \frac{2\lambda}{\lambda_0^2}\frac{I_1(\lambda)}{I_0(\lambda_0)+I_1(\lambda_0)}, && y\leqslant y_0\\ \frac{hU}{h_{e0}Ft} &= \frac{2}{\lambda_0}\frac{I_1(\lambda_0)}{I_0(\lambda_0)+I_1(\lambda_0)}\exp\left(-\frac{y-y_0}{R}\right), && y\geqslant y_0\end{aligned}\right\}. \tag{17}$$

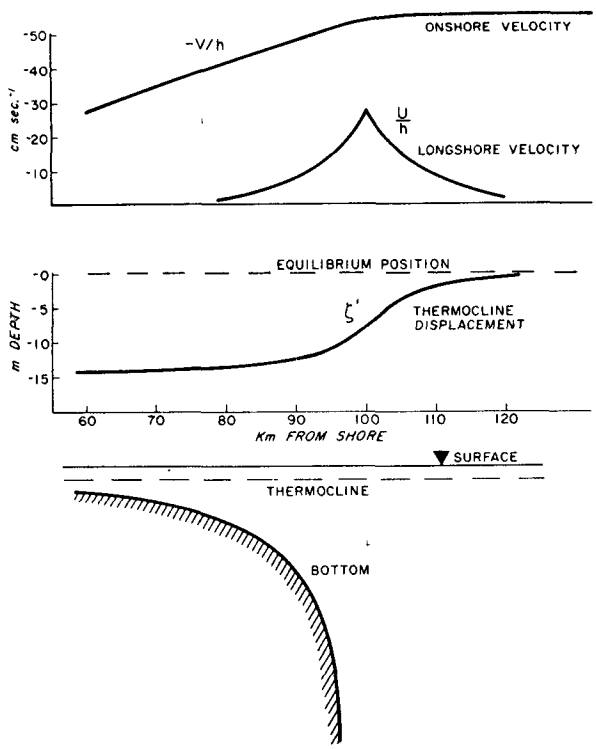

FIG. 4. "Shelf jet" and thermocline displacements generated by a shore-parallel wind.

These results are illustrated in Fig. 4, for the example quoted above and again with a wind stress of 10 dyn cm^{-2}, for $t=10^5$ sec (27.7 hr) after the imposition of the wind stress. Observe that the amplitudes of ζ' and U increase linearly with time, as in other coastal jet-development problems. The onshore velocity remains constant, being equal to the Ekman drift far offshore, and reducing gradually toward the shore exactly as the longshore velocity was in the example with an onshore wind. The thermocline topography is also similar to the earlier example, although the displacements are now very much larger (and growing linearly with time). At the amplitude illustrated (14 m over the shelf) the validity of the linear theory is already quite doubtful, given a 20 m equilibrium thermocline depth. The jet accompanying these large thermocline displacements is of modest amplitude, the top speed being 27 cm sec^{-1}. For a similar wind stress impulse, theoretically-predicted *coastal* jet amplitudes are generally much larger. Thus, what we might describe as the "shelf jet" is a rather less striking phenomenon, although still likely to be easily observable. We note that the longshore velocity in this example is what would be calculated from the thermocline topography, assuming geostrophic balance, the wind stress being balanced by Ekman drift.

Weak step-like features on the σ_t-surfaces under summer conditions over the edge of the shelf are discernible in the sections published by Ketchum and Corwin (1964) and Creswell (1967), for example. No direct current measurements at all seem to be available with which the theory could be compared, nor are hydrographic stations ordinarily taken detailed enough to resolve the shelf region adequately, in such a way that at least the effects of wind stress impulses on pycnocline topography could be analyzed.

The question may be asked as to what extent the results obtained above depend on the discontinuity in slope assumed at the shelf break in the idealized shelf model, and whether a smooth h_e distribution would not completely obliterate the shelf jet. To answer this, we observe that a (numerical) solution of Eq. (6) may be obtained for an arbitrary $h_e(y)$ distribution. *Asymptotically*, for small and large y, respectively, any realistic depth distribution will yield Eqs. (7). Therefore, Eqs. (8) and (10) are the solutions of Eq. (6) for small and large y, respectively, given an arbitrary $h_e(y)$. It follows that the distribution of longshore velocities, etc., which we have calculated will model the general character of the forced response correctly, although the details at the shelf-break region are likely to show discrepancies (e.g., the cusp in the U-distribution in Fig. 4 is certain to be smoothed out by any "real" topography). Similar conclusions follow from a comparison of the above results with those of O'Brien and Hurlburt (1972), and the other numerical studies already referred to in the introduction.

Acknowledgments. This work was supported by the Office of Naval Research under Contract N00014-66-CO241: NR 083-004. I am indebted to Prof. H. Stommel of the Massachusetts Institute of Technology and to W. R. Wright and G. Volkmann of the Woods Hole Oceanographic Institution for discussions of the shelf region.

REFERENCES

Crépon, M., 1967: Hydrodynamique marine en regime impulsionnel. *Cah. Oceanogr.*, **19**, 847–880.

Creswell, G. M., 1967: Quasi-synoptic montly hydrography of the transition region between coastal and slope water south of Cape Cod, Mass. Unpubl. ms., W.H.O.I. Ref. 67–35.

Csanady, G. T., 1971: Baroclinic boundary currents and long edge-waves in basins with sloping shores. *J. Phys. Oceanogr.*, **1**, 92–104.

——, 1973: Transverse internal seiches in large, oblong lakes and marginal seas. W.H.O.I. Contribution No. 3043.

Hurlburt, H. E., and J. D. Thompson, 1973: Coastal upwelling on a β-plane. *J. Phys. Oceanogr.*, **3**, 16–32.

Ketchum, B. H., and N. Corwin, 1964: The persistence of "winter" water on the continental shelf south of Long Island, New York. *Limnol. Oceanogr.*, **9**, 467–475.

O'Brien, J. J., and H. E. Hurlburt, 1972: A numerical model of coastal upwelling. *J. Phys. Oceanogr.*, **2**, 14–26.

Thompson, J. D., and J. J. O'Brien, 1973: Time-dependent coastal upwelling. *J. Phys. Oceanogr.*, **3**, 33–46.